# Comprehensive Analysis of Analogs of Amine-Related Psychoactive Substances Using Femtosecond Laser Ionization Mass Spectrometry

Siddihalu, Lakshitha Madunil
Faculty of Design, Kyushu University

Imasaka, Totaro
Kyushu University

Imasaka, Tomoko
Faculty of Design, Kyushu University



出版情報：Journal of the American Society for Mass Spectrometry. 33 (1), pp.90-99, 2022-01-05. American Chemical Society
バージョン：

ACS Partner Journal

Journal of the American Society for Mass Spectrometry

pubs.acs.org/jasms

Research Article

# Comprehensive Analysis of Analogues of Amine-Related Psychoactive Substances Using Femtosecond Laser Ionization Mass Spectrometry

Siddihalu Lakshitha Madunil, Totaro Imasaka, and Tomoko Imasaka*

Cite This: *J. Am. Soc. Mass Spectrom.* 2022, 33, 90−99

Read Online

ACCESS | Metrics & More | Article Recommendations | Supporting Information

**ABSTRACT:** Amine-related psychoactive molecules contain N−$C_\alpha$ and $C_\alpha$−$C_\beta$ bonds, which easily dissociate to form various fragment ions in electron ionization mass spectrometry (EIMS). Therefore, observing a molecular ion and then determining the molecular weight of the analyte is difficult. In this study, we examined phenethylamine, 3,4-methylenedioxyphenethylamine, tryptamine, *N*-methylephedrine, and nicotine as well as analogues of amine-related psychoactive substances using EIMS and femtosecond laser ionization mass spectrometry (fs-LIMS) combined with gas chromatography for comprehensive analysis. A molecular ion was clearly observed in fs-LIMS for all of these compounds, which was in contrast to EIMS providing fragment ions dominantly (no molecular ion was observed for *N*-methylephedrine). This favorable result was obtained by adjusting the laser wavelength to the optimal value for two-photon ionization to minimize the excess energy remaining in the molecular ion. It therefore appears that fs-LIMS is superior to EIMS in terms of observing a molecular ion and would be potentially useful for identifying a variety of amine-related psychoactive substances, some of which are illegal and are of interest in the field of forensic science.

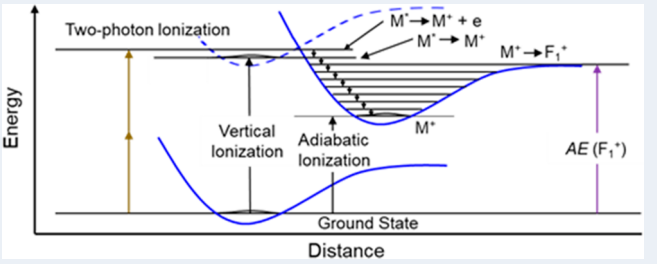


**KEYWORDS:** *femtosecond laser, multiphoton ionization, mass spectrometry, psychoactive substances, fragmentation process*

## INTRODUCTION

Many types of psychoactive substances have been available on illegal drug markets over the past decades. In fact, more than 270 million individuals used drugs of abuse in 2018.[1] Hundreds of new drugs are synthesized by criminals every year, and some of them have been shown to have unpredictable effects with severe health consequences. These widely used psychoactive substances include opiates, amphetamines, tryptamines, and norpseudoephedrines, to name a few.[2]

Because these compounds have societal importance, an accurate and reliable analytical method for determining such psychoactive substances is highly desirable. A variety of analytical methods have been developed to identify the drugs and include gas chromatography combined with vacuum ultraviolet spectroscopy (VUV), infrared spectroscopy (IR), and nuclear magnetic resonance spectrometry (NMR).[3−8] These methods all have their pros and cons depending on the application. It should be noted that law enforcement authorities need to make important decisions based on scientific proof in cases of incidents that involve the use of such drugs.[9] Therefore, a comprehensive method, e.g., a high-resolution separation technique combined with a sensitive/selective spectrometric technique, is essential for obtaining reliable scientific evidence for use in a court of law.[10] The most popular method for achieving this is gas chromatography combined with mass spectrometry (GC−MS). The sample can be separated by liquid chromatography (LC) and measured by electrospray ionization-MS × MS (the isomers were differentiated by the statistical/chemometric analysis of the fragment ions).[11−13] However, the separation resolution of LC is sometimes insufficient and is not suitable for comprehensive analysis of unknown samples since the target analyte should be decided before measuring the sample.

A fragmentation pattern in the mass spectrum provides a useful means for structural analysis even for an unknown chemical species. However, typical aliphatic amines easily dissociate to form many fragment ions via various pathways, i.e., by cleavage of N−$C_\alpha$ and $C_\alpha$−$C_\beta$ bonds in the molecule, thus making the identification of closely related analogues difficult. In addition, a rearrangement assisted by a lone pair of electrons on the nitrogen atom occurs efficiently during the ionization/fragmentation process, which makes the structural analysis even more difficult. When no standard reference

Received: September 9, 2021
Revised: November 18, 2021
Accepted: November 19, 2021
Published: November 30, 2021

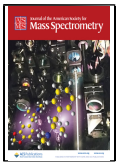

material is available or when a new compound is synthesized and used, it is difficult to assign the compound using the GC and MS database. As a result, it is necessary to assign the analyte from the molecular weight derived from a molecular ion and from the fragmenation pattern in the mass spectrum. In electron ionization mass spectrometry (EIMS), fragmentation is the dominant process and large fragment ions are seldom observed, which makes the identification of an unknown chemical species difficult. Thus, it would be desirable to develop a new type of MS that permits the observation of a molecular ion as well as large fragment ions especially for isomer analysis. It should be noted that the fragmentation can be suppressed in cold-EIMS, in which a analyte molecule is cooled by supersonic jet expansion into a vacuum to decrease the internal energy.[14−16] The fragmentation can be reduced by decreasing the ionization energy from 70 to 10 eV.[17]

Photoionization has been developed as a new technique for soft ionization in MS.[18,19] Photodissociation dynamics and ionization efficiency have been studied using a variety of pulse lasers as the ionization sources.[20−23] A technique based on single photon nanosecond/femtosecond ionization is developed to enhance a molecular ion.[24,25] A hydrogen laser (ca. 8 eV) has been employed for this purpose.[26] A tunable nanosecond laser provides an advantage for selective ionization because of a narrow spectral line width, since a molecule can be excited to a specified level by absorbing the first photon and subsequently ionized by absorbing an additional photon, as shown in Figure 1a. However, this scheme of resonance-

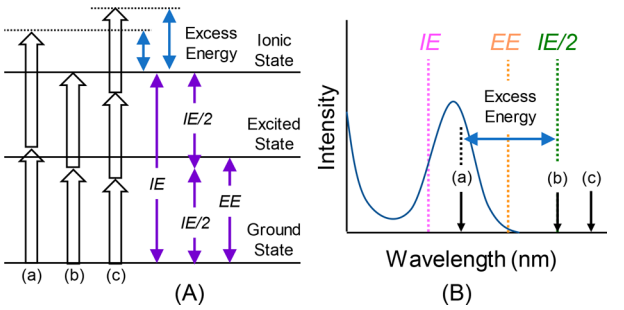


**Figure 1.** (A) Scheme of ionization processes; (B) schematic absorption spectrum. IE, ionization energy; IE/2, half of the ionization energy; EE, excitation energy. (a) Resonance-enhanced two-photon ionization, (b) nonresonant two-photon ionization, and (c) nonresonant three-photon ionization.

enhanced two-photon ionization (RE2PI) has an unavoidable limitation. For example, when the absorption band is located at above the half value of the ionization energy (IE), the excess energy increases and accelerates the fragmentation. This problem can be overcome by ionizing a molecule through a virtual state (see Figure 1b)), which is referred to as nonresonant two-photon ionization (NR2PI). In this case, the excess energy can be reduced to zero by adjusting the laser wavelength at the half of the IE. Unfortunately, the efficiency of NR2PI is generally lower than that of RE2PI. To solve this problem, a femtosecond laser can be used for ionization.[27−30] The efficiency can be increased to a level comparable to that of RE2PI by reducing the laser pulse width to <50 fs. When the wavelength of the laser is located at longer wavelength (see Figure 1c), three photons are required for ionization that drastically increases the excess energy remaining in a molecular ion and seriously accelerates fragmentation. This technique of multiphoton ionization (MPI) has been combined with time-of-flight mass spectrometry (TOFMS) and has been applied to analyses of a variety of compounds, e.g., triacetone triperoxide, 4-methylcyclohexanols, and organochlorine pesticides.[30−33] It should be noted that polycyclic aromatic hydrocarbons can be measured at subfemtogram levels, which is a few orders of magnitude better than with conventional MS.[34]

As discussed above, a psychoactive substance with an aliphatic amine chain is prone to dominantly produce fragment ions, and the molecular ion signal is weak or sometimes missing in EIMS.[35,36] A basic study of the fragmentation pathways of analogues of such molecules could be useful for the assignment of closely related drugs of abuse that cannot be measured by law in an academic laboratory. As shown in Figure 2, commercially available phenethylamine is an analogue of amphetamine and methylamphetamine, which are stimulants that are frequently found in illegal drugs. Note that the chemcial sturcture of 3,4-methylenedioxyphenethylamine is very similar to that of both 3,4-methylenedioxymethamphetamine (MDMA) and 3,4-methylenedioxyamphet-

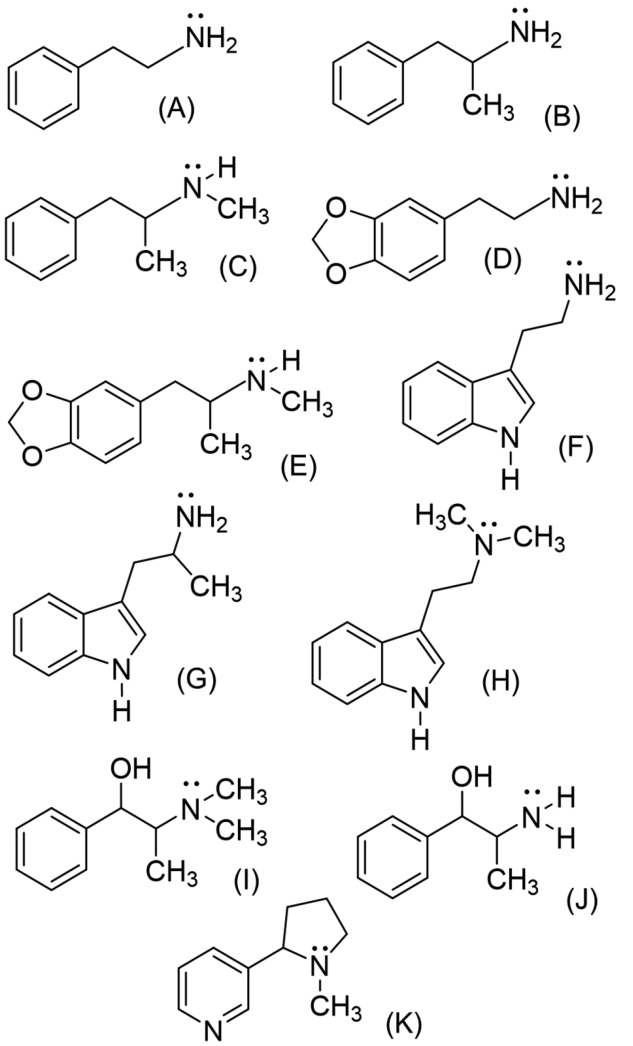


**Figure 2.** Chemical structures of amine-related psychoactive substances and their analogues: (A) phenethylamine, (B) amphetamine, (C) methylamphetamine, (D) 3,4-methylenedioxyphenethylamine, (E) MDMA, (F) tryptamine, (G) AMT, (H) DMT, (I) *N*-methylephedrine, (J) cathine, and (K) nicotine.



https://doi.org/10.1021/jasms.1c00282
J. Am. Soc. Mass Spectrom. 2022, 33, 90−99

amine (MDA). In addition, many tryptamine derivatives have been employed as hallucinogens, e.g., α-methyltryptamine (AMT), *N,N*-dimethyltryptamine (DMT), as well as 5-methoxy-α-methyltryptamine (α-O), and *N,N*-diethyltryptamine (DET). Moreover, *N*-methylephedrine has the same chemical structure as cathine, a psychoactive substance, except for the fact that the nitrogen atom contains attached methyl groups. Note that nicotine is an amine-related compound and is well known as a health hazard substance, although it is not categorized as a drug of abuse.

In this study, we examined some analogues of amine-related psychoactive substances by GC−MS using a femtosecond laser as the ionization source in MS (fs-LIMS). Figure 3 shows a

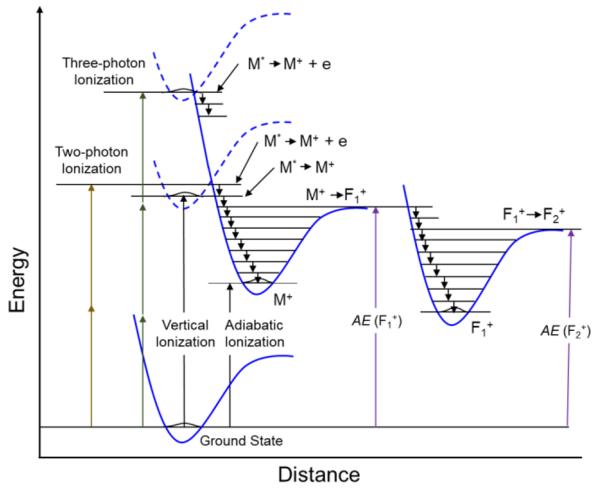


**Figure 3.** Energy diagram for the ionization of a molecule. M*, superexcited state; $M^+$, molecular ion; e, electron; $F^+$, fragment ion; AE, appearance energy.

possible ionization mechanism for amine-related psychoactive substances and their analogues. The thermal energy spread in the ground state ($\sim kT$) was calculated to be 0.026 eV at room temperature, where $k$ is the Boltzmann constant and $T$ is the absolute temperature. This value is smaller than the line width (full width at half-maximum, fwhm) of the femtosecond laser (0.052 eV) and can be negligible in the discussion of the ionization process. There are possible two major ionization pathways, i.e., two-photon and three-photon ionization processes. In this scheme, a molecule in the ground state is excited to a superexcited state, M*, by absorbing two or three photons. When the total energy of two (or three) photons is identical to the value of "adiabatic ionization", the molecule is ionized to produce a molecular ion with no internal energy and an electron with no kinetic energy. This phenomenon is efficient and can be easily observed when the ionic state has a configuration similar to that of the neutral one, especially for a rigid molecule such as an aromatic hydrocarbon. In fact, this process has been measured by photoelectron−photoion coincidence (PEPICO) spectroscopy,[37,38] in which only the ion formed by emitting a zero-kinetic-energy electron can be detected using a tunable VUV light source. However, this process is inefficient in the case of a flexible molecule such as amine-related drugs and their analogues due to a small Franck−Condon factor. As a result, the contribution of adiabatic ionization is small, and fragment ions are the dominant species for amine-related compounds. When the internal energy in the superexcited state is larger than the value (IE) of "vertical ionization", the molecule ejects an electron and is ionized to produce a molecular ion. The internal energy in the molecular ion is then redistributed to vibrational energies along numerous different coordinates by internal conversion. Accordingly, a stable molecular ion with a large internal energy is formed and can be observed in the mass spectrum. When the excess energy remaining in the molecular ion, $M^+$, is larger than the dissociation limit, a fragment ion, $F_1^+$, is formed. A minimum energy to observe $F_1^+$ is referred to as "appearance energy AE ($F_1^+$)". In the same manner, the fragment ion, $F_2^+$, is formed from $F_1^+$. The minimum energy is referred to as "appearance energy AE ($F_2^+$)".

As mentioned, the molecular ion is produced efficiently via RE2PI/NR2PI at or slightly above the IE and tends to dissociate at shorter wavelengths with an increase in excess energy (see Figure 1). On the other hand, when the two-photon energy is smaller than the IE, three photons are required for ionization, resulting in a large excess energy and dominant fragmentation. Therefore, carefully optimizing the laser wavelength for observing a molecular ion as well as large fragment ions is highly desirable, especially for isomer analysis. In EI, the excess energy cannot be controlled due to an elastic collision of electrons, and as a result, it is difficult to minimize the excess energy and to suppress the fragmentation. As demonstrated in this study, a molecular ion as well as large fragment ions were enhanced significantly in fs-LIMS when the laser wavelength was optimized to minimize the excess energy in the molecular ion. The fragmentation patterns were also examined in an attempt to reliably assign amine-related psychoactive substances that are measured in forensic science.

## EXPERIMENTAL SECTION

**GC/MPI-TOFMS.** A 1 μL aliquot of a 20 μg $mL^{-1}$ solution of each sample was injected into a GC (6890 N, Agilent Technologies, Santa Clara, CA) using an autosampler (7683B, Agilent Technologies). Note that the sample was prepared at a high concentration because of a low output power of a tunable femtosecond ultraviolet (UV) laser for use in basic studies. The analytes were separated by a DB-5 ms column (length 30 m, inner diameter 0.25 mm, film thickness 0.25 μm). The initial temperature of the capillary column was 50 °C and was held for 1 min, a ramp of 25 °C $min^{-1}$ to 125 °C, and held for 1 min, after which the temperature was increased to 140 °C at a rate of 4 °C $min^{-1}$ and was held for 1 min. Finally, the temperature was increased to 300 °C at a rate of 4 °C $min^{-1}$ and held for 2 min. Helium was used as a carrier gas at a flow rate of 1.0 mL $min^{-1}$. The analytes eluting from the column were measured by a linear-type TOFMS (mass resolution, $m/\Delta m$ = 1500) developed in this laboratory.[18,19] An assembly of microchannel plates (F4655-11, Hamamatsu Photonics, Shizuoka, Japan) was used as an ion detector. The temperature of a GC inlet as well as the interface between the GC and the MS was kept at 250 °C for a sample containing phenethylamine, 3,4-metylenedioxyphenethylamine, tryptamine, and nicotine, while the temperatures were decreased to 200 °C for a sample containing *N*-methylephedrine (and nicotine) to reduce thermal decomposition. The ion signal was recorded by a digitizer (Acqiris AP240, Agilent Technologies). Two-dimensional data of GC−MS were displayed using a software program developed in the laboratory. An optical parametric amplifier (OPA, TOPAS, Spectra-Physics, Santa Clara, CA) pumped by a Ti:sapphire laser (TS, 800 nm, 35 fs, 1 kHz, 6 mJ, Solstice Ace, Spectra-Physics) was used as a tunable laser


https://doi.org/10.1021/jasms.1c00282
J. Am. Soc. Mass Spectrom. 2022, 33, 90−99

source in the near-infrared region, the frequency of which was converted into the UV region of 250−330 nm using a UV option of the OPA for use as the ionization source (5−20 mW; pulse duration, not measured). The temperature of the sample inlet port and the temperature program of GC−EIMS (GCMS-QP2010, Shimadzu, Kyoto, Japan) were identical to those used in GC−LIMS. The ion source temperature was adjusted at 200 °C.

**Reagents.** Standard samples of phenethylamine (molecular weight, 121.2) and tryptamine (160.2) were purchased from Wako Chemical Industries, Tokyo, Japan, and *N*-methylephedrine (179.3) and nicotine (162.2) from Sigma-Aldrich Japan, while 3,4-methylenedioxyphenethylamine (165.2) was supplied from Combi-Blocks, San Diego, CA. Methanol (GC−MS grade) used as a solvent was purchased from Sigma-Aldrich Japan. The chemical structures of these compounds are shown in Figure 2.

**Computational Methods.** Quantum chemical calculations were performed in order to find the optimum wavelength for ionization using the Gaussian 16 program. Minimum geometries were obtained using the B3LYP method, based on density functional theory (DFT) with a cc-pVDZ basis set. Actually, the B3LYP/cc-pVTZ method was used to evaluate the vertical ionization energy, which was calculated from the difference between the energies of the ground and ionic states.[39] The lowest 100 singlet transition energies and the oscillator strengths were calculated using time-dependent DFT (TD-DFT). The absorption spectrum was predicted for neutral and ionic species by calculating the envelope of the transitions using the GaussView 5 software program. They are used for the discussion of autodissociation and photodissociation from the ionic state (see the Phenethylamine section). The computed data are shown in Figures S1−S10 in the Supporting Information. It is necessary to decrease the excess energy for observing a molecular ion and large fragment ions as well (see Figures 1 and 3 and their captions).

## RESULTS AND DISCUSSION

**Two-Dimensional Display.** A sample mixture containing phenethylamine, 3,4-methylenedioxyphenethylamine, tryptamine, and nicotine was separated by GC and measured by fs-LIMS. Figure 4 shows the two-dimensional display of the GC−MS measured for this sample (data for a sample mixture containing *N*-methylephedrine and nicotine are shown in Figure S11). A molecular ion was observed for all of the compounds measured at 290 nm (the mass spectra measured at different wavelengths are shown in Figures S12−S16). A small fragment ion of $(M - 1)^+$ was clearly observed, indicating that the mass resolution was sufficient for discussing the fragmentation. It should be noted that the fragmentation pattern of phenethylamine ($m/z$ = 121) is very similar to that of phenyl oxirane ($m/z$ = 120) except for a molecular ion, as reported in the NIST EIMS database.[40] As a result, observing a molecular ion and sufficient mass resolution are required for these compounds to be differentiated. The chromatogram signal left trails for two compounds eluting later, which was suspected to arise from the high polarities (low volatility) of these compounds. This unfavorable result can be avoided by increasing the temperature of the separation column, although the components eluting earlier would decompose in the sample injection port and also on the GC column. In fact, a sample mixture containing *N*-methylephedrine (and nicotine) was measured at lower temperature (see the Experimental Section and Figure S11).

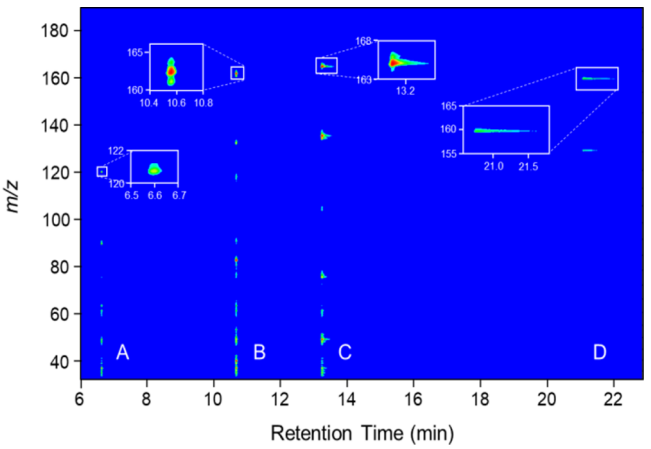


**Figure 4.** Two-dimensional display of a GC−MS spectrum measured at 290 nm for a sample mixture containing (A) phenethylamine, (B) nicotine, (C) 3,4-methylenedioxyphenethylamine, and (D) tryptamine. A part indicating a molecular ion is expanded and is shown as an inset.

**Phenethylamine.** Figure 5A shows the mass spectrum of phenethylamine measured by EIMS. The molecular ion signal

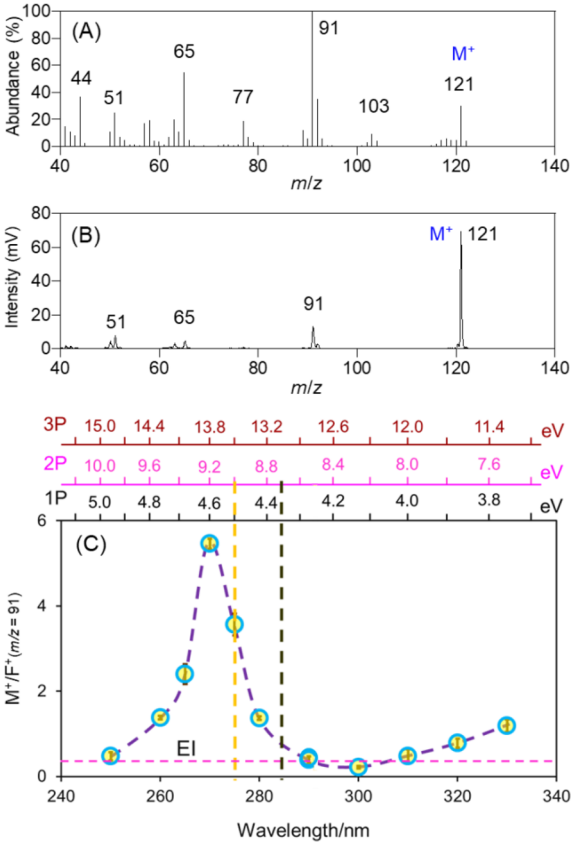


**Figure 5.** Mass spectral data for phenethylamine: (A) EIMS, (B) fs-LIMS measured at 270 nm, (C) ratio of signal intensities observed for a molecular ion, $M^+$, and a fragment ion $(C_7H_7)^+$ ($m/z$ = 91) at different wavelengths (the errors in the observed data are shown in the figure). The ratio obtained by EIMS is shown as a pink broken line. Yellow broken line: IE measured by photoelectron spectroscopy. Dark brown broken line: IE calculated by DFT.



https://doi.org/10.1021/jasms.1c00282
J. Am. Soc. Mass Spectrom. 2022, 33, 90−99

Table 1. Ratio of Signal Intensities, $M^+/F^+$, Observed for Analogues of Amine-Related Psychoactive Substances[a]

| | techniques | $M^+/F^+$ | EF | obsd maximum | $IE_{obs}$, $IE_{cal}$ |
|---|---|---|---|---|---|
| phenethylamine | EI (70 eV) | 0.3 | | | 8.99, 8.73 |
| | UV 2PI (270 nm, 9.18 eV) | 5.46 ± 0.11 | 18 | 9.18 | |
| 3,4-methylenedioxyphenethylamine | EI (70 eV) | 0.18 | | | −, 7.71 |
| | UV 2PI (300 nm, 8.27 eV) | 2.19 ± 0.21 | 12 | 8.41 | |
| tryptamine | EI (70 eV) | 0.15 | | | 7.69, 7.48 |
| | UV 2PI (290 nm, 8.85 eV) | 4.15 ± 0.32 | 28 | 8.54 | |
| *N*-methylephedrine | EI (70 eV) | ND | | | −, 8.30 |
| | UV 2PI (280 nm, 8.86 eV) | 2.0 ± 0.13 | − | 8.86 | |
| nicotine | EI (70 eV) | 0.12 | | | 8.23, 8.41 |
| | UV 2PI (290 nm, 8.85 eV) | 0.92 ± 0.06 | 7.8 | 8.54 | |

[a]ND: not detected. $F^+$: base peak in EIMS (except for *N*-methylephedrine, see the caption of Figure 7). EF: enhancement factor. Observed maximum: the energy (eV) corresponding to the optimal wavelength for observing a molecular ion in fs-LIMS. $IE_{obs}$ and $IE_{cal}$: the ionization energies (eV) reported in the reference and calculated by DFT in this study, respectively.

observed at $m/z$ = 121 was weak, and several large fragment ions were observed in the mass spectrum. Because phenethylamine has carbon atoms at the $\alpha$- and $\beta$-positions in the amine chain (see Figure S17), there are two major pathways for the dissociation of the molecular ion, i.e., cleavages at $C_\alpha$−N and $C_\alpha$−$C_\beta$ bonds.[41] A signal at $m/z$ = 103 suggests the formation of $(M - NH_3 - H)^+$. Note that the signal at $m/z$ = 91 was observed as a base peak, suggesting that a $CH_2NH_2$ group dissociated to form a stable tropylium ion $(C_7H_7)^+$ or that a $CH_2NH$ group dissociated followed by the subsequent dissociation of a hydrogen atom. The other large peaks were a benzene cation ($m/z$ = 77), a cyclopentadienyl cation ($m/z$ = 65), a cyclobutadienyl cation ($m/z$ = 51), and $(CH_3CH{=}NH_2)^+$ ($m/z$ = 44). This fragmentation pathway is important in terms of recognizing analogues of compounds such as amphetamine and methylamphetamine.

Figure 5B shows a mass spectrum measured by fs-LIMS. A large molecular ion ($m/z$ = 121) was observed as a base peak at 270 nm. A signal at $m/z$ = 103 was missing in the mass spectrum, suggesting that fragmentation at the N−$C_\alpha$ bond had been suppressed. On the other hand, a peak at $m/z$ = 91 was observed but the signal intensity was smaller than the molecular ion. Note that the ratio of the signal intensities at $m/z$ = 91 and 92 measured by fs-LIMS was larger than the ratio measured by EI. This suggests that a tropylium ion ($m/z$ = 91) is more efficiently produced by decreasing the excess energy in the ionic state by fs-LIMS.

Figure 5C shows the ratio of the molecular ion and the fragment ion, $M^+/F^+$ ($m/z$ = 91), measured at different wavelength, indicating that the intensity of the molecular ion can be enhanced significantly when the wavelength is carefully adjusted at the optimal value (270 nm or 9.18 eV). The IE value was calculated to be 8.73 eV by DFT and was measured by photoelectron spectroscopy and reported to be 8.99 eV.[42] The two-photon energy at the maximum of the signal (9.18 eV) was slightly larger than these values, suggesting that an energy larger than the IE is necessary for achieving efficient ionization and that even a small excess energy (ca. 0.2 eV) accelerates dissociation of a molecular ion, as was previously reported for 4-methylcyclohexanols.[32] This result indicates that phenethylamine is very amenable to undergoing dissociation, probably due to the presence of an aliphatic amine chain. It should be noted that the ratio of $M^+/F^+$ ($m/z$ = 91) decreases rapidly at longer wavelengths. This unfavorable result can be explained by three-photon ionization (3PI), significantly increasing the excess energy in the molecular ion (see Figure 1). As shown in Figure S1, there is no absorption band for the molecule in the spectral region from 250 to 330 nm, i.e., NR2PI or NR3PI. Note that the molar absorptivity (ca. $1 \times 10^3$ $mol^{-1}cm^{-1}$) (see Figure S2) suggests that there are two possible processes for producing fragment ions via NR3PI, i.e., autodissociation induced by direct three-photon absorption and photodissociation induced by two-photon absorption followed by the absorption of another photon from the ionic state. The excess energy in NR3PI varies from 4.1 to 2.5 eV in the spectral region from 290 to 330 nm. It has been reported that the molecular ion dissociates efficiently when the excess energy is larger than 3 eV.[29,31,32] It is interesting to note that the ratio of $M^+/F^+$ ($m/z$ = 91) observed at 300 nm is smaller than the value obtained by EI, suggesting that the excess energy (3.7 = 12.4 − (8.99 + 8.5)/2 eV) at 300 nm by NR3PI is larger than the excess energy available at 70 eV in EI.

In this study, phenethylamine was used as an analogue of amphetamine and methylamphetamine, i.e., stimulants, that are currently found in illegal drugs. The difference in chemical structure is only one methyl group substituted at the $C_\alpha$ atom for amphetamine and an additional methyl group at the nitrogen atom (see Figure 2). As shown in Table 1, the ratios of the values, $M^+/F^+$ ($m/z$ = 91), obtained based on EI and NR2PI were 0.30 to 5.46 ± 0.11, respectively. Accordingly, the relative signal intensity of the molecular ion can be enhanced by 18-fold (enhancement factor = 18). The fragmentation pathways for amphetamine and methylamphetamine are summarized in Figures S18 and S19, respectively, and are similar to that of phenethylamine (cf. Figure S17). As reported in the NIST EIMS database, the ratio of $M^+/F^+$ is small for both amphetamine (ca. 0.05) and methylamphetamine (ca. 0.10).[43,44] Therefore, finding a molecular ion in EIMS for these compounds in a complex matrix would not be easy. Thus, fs-LIMS providing a molecular ion as the major signal would have a substantial advantage over EIMS.

**3,4-Methylenedioxyphenethylamine.** Figure 6A shows the mass spectrum of 3,4-methylenedioxyphenethylamine measured by EIMS. The signal intensity of the molecular ion ($m/z$ = 165) was 18% of the base peak observed at $m/z$ = 136. Very similar fragment patterns have been reported for compounds with a 3,4-methylenedioxy group such as 3,4-methylenedioxytoluene and related compounds with a benzaldehyde group such as 3-methoxybenzaldehyde in the NIST EIMS database.[45,46] The fragmentation pathway of 3,4-methylenedioxyphenethylamine is summarized in Figure S20. The signal observed at $m/z$ = 136 was caused by cleavage of


https://doi.org/10.1021/jasms.1c00282
J. Am. Soc. Mass Spectrom. 2022, 33, 90−99

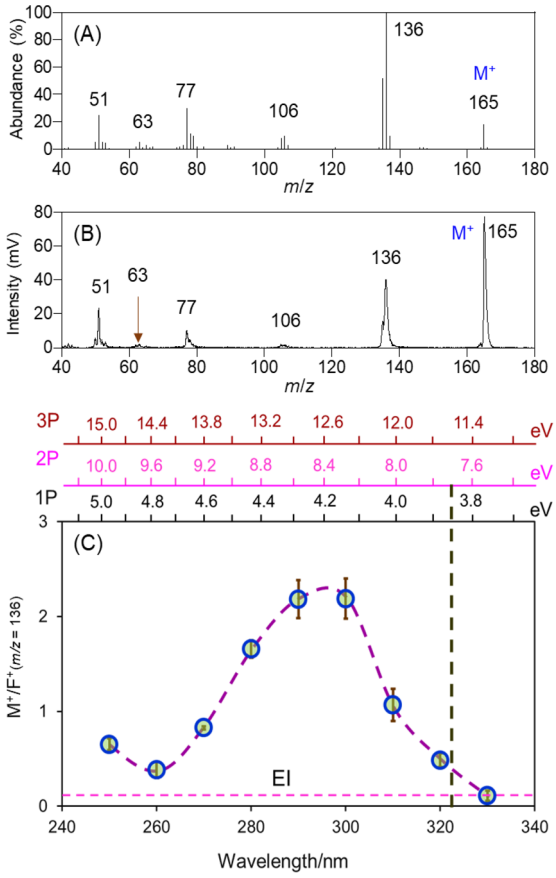


**Figure 6.** Mass spectral data for 3,4-methylenedioxyphenethylamine: (A) EIMS, (B) fs-LIMS measured at 300 nm, (C) ratio of the signal intensities observed for a molecular ion, $M^+$, and a fragment ion, $(M - CHNH_2)^+$ ($m/z$ = 136), at different wavelengths. The ratio obtained by EIMS is shown as a pink broken line. No data were available for IE measured by photoelectron spectroscopy. Dark brown broken line: IE calculated by DFT.

the $C_\alpha$–$C_\beta$ bond and the further dissociation of this fragment ion to a smaller fragment ion ($m/z$ = 106) by a rearrangement followed by a ring cleavage of the methylenedioxy group. Finally, the ion was converted into a benzene cation ($m/z$ = 77), a 1-cyclopenten-4-yn-1-yl cation ($m/z$ = 63), and a cyclobutadienyl cation ($m/z$ = 51). This type of pathway is common for compounds with a 3,4-methylenedioxy group such as MDMA except for a large signal corresponding to $(CH_3CH{=}NH(CH_3))^+$ ($m/z$ = 58) (see Figures S20 and S21 and the NIST database of MDMA) which corresponds to $(CH_2{=}NH_2)^+$ ($m/z$ = 30) for 3,4-methylenedioxyphenethylamine (not shown in Figure 6A).

In fs-LIMS, a large molecular ion signal was observed at $m/z$ = 165 as a base peak when measured at 290 nm, as shown in Figure 6B. A fragment pattern similar to EIMS was observed in the data. The dependence of the $M^+/F^+$ ($m/z$ = 136) ratio on the laser wavelength is shown in Figure 6C. The maximal value was observed at around 295 nm (8.41 eV). The IE value of this compound was calculated to be 7.71 eV by DFT (no observed value was available). The intense molecular ion signal can be explained by a small excess energy (0.7 = 8.41−7.71 eV) in NR2PI. As discussed above, the ratio decreased at shorter wavelengths with a gradual increase in excess energy by NR2PI and decreased significantly at longer wavelengths with a substantial increase in excess energy by NR3PI. The increase in the ratio at <250 nm can be attributed to a resonance effect (RE2PI), since the molar absorptivity increases at shorter wavelengths from 250 nm ($5 \times 10^3$ $mol^{-1}$ $cm^{-1}$ at 250 nm, see Figure S3).

The 3,4-methylenedioxyphenethylamine molecule is an analogue of MDMA. As discussed above, the fragmentation pathways for these two compounds are very similar (see Figures S20 and S21). As shown in Table 1, the relative intensity of the molecular ion signal can be enhanced 12-fold by fs-LIMS compared with EIMS. Unfortunately, no data were available for 3,4-methylenedioxyphenethylamine in the NIST EIMS database, and as a result, it was difficult to compare the EIMS data for these compounds.[47] However, the substitution of a methyl group at the nitrogen atom (i.e., DMT) increased the ratio by 2.5-fold and substitution of a methyl group at the $C_\beta$ atom (i.e., AMT) increased the ratio by 24-fold in the case of tryptamine.[48,49] These data suggest that the substitution of methyl groups from this compound to form MDMA would decrease the ratio 9.6-fold (= 24/2.5). Since a molecular ion was clearly observed as a base peak for 3,4-methylenedioxyphenethylamine, as shown in Figure 6B, a molecular ion would likely be observed for MDMA in fs-LIMS.

**Tryptamine.** Figure 7A shows the mass spectrum of tryptamine measured by EIMS. The signal intensity of the

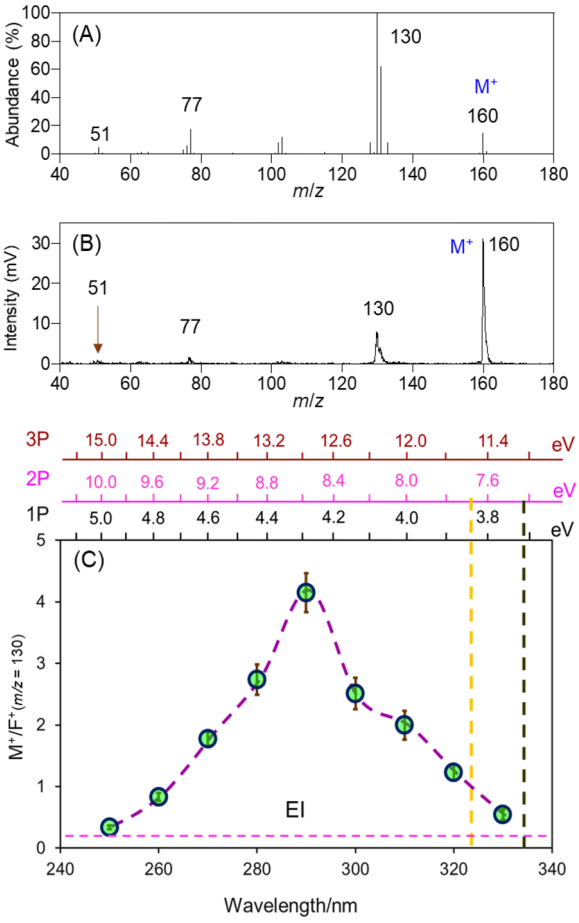


**Figure 7.** Mass spectral data of tryptamine: (A) EIMS, (B) fs-LIMS measured at 290 nm, (C) ratio of the signal intensities observed for a molecular ion, $M^+$, and a fragment ion $(M\text{-}CH_2NH_2)^+$ ($m/z$ = 130) at different wavelengths. The ratio obtained by EIMS is shown as a pink broken line. Yellow broken line: IE measured by photoelectron spectroscopy. Dark brown broken line: IE calculated by DFT.



https://doi.org/10.1021/jasms.1c00282
J. Am. Soc. Mass Spectrom. 2022, 33, 90−99

molecular ion ($m/z$ = 160) was 15% of the base peak observed at $m/z$ = 130. The fragment pattern is very similar to that for other indole derivatives such as 3-methylindole and 2-methylindole reported in the NIST EIMS database.[50,51] Furthermore, observing a molecular ion is important for the assignment of this compound. The base peak can arise from a cleavage of the $C_\alpha$–$C_\beta$ bond, as shown in Figure S22. This fragment dissociates into an indole cation ($m/z$ = 117) and a benzene cation ($m/z$ = 77). A similar dissociation pathway can be considered for AMT and DMT (see Figures S23 and S24).

As shown in Figure 7B, a large molecular ion was clearly observed as a base peak in fs-LIMS, in addition to a few small fragment ions, when measured at 290 nm. The dependence of the ratio, $M^+/F^+$ ($m/z$ = 130), on the laser wavelength is shown in Figure 7C. The absorption spectrum calculated by TD-DFT is extended to 280 nm at shorter wavelengths (see Figure S5), and the absorption spectrum of indole, a chromophore of tryptamine, appears, even at 300 nm, in the NIST database,[52] suggesting that this compound can be ionized via RE2PI at <300 nm (the spectrum calculated by TD-DFT is usually shifted to shorter wavelengths). The maximum value was observed at 8.54 eV, which was considerably larger than the adiabatic ionization energy of 7.69 eV, as measured by photoelectron spectroscopy.[42] The calculated excess energy was 1.06 eV (= 8.54−7.48 eV) at the optimal wavelength of 290 nm, suggesting that the molecular ion of tryptamine is stabilized by an indole chromophore, which contains a larger number of $\pi$ electrons.

Tryptamine is an analogue of AMT and DMT, which are referred to as hallucinogens or psychedelics. The molecular ions of these compounds, as listed in the NIST EIMS database, are weak (ca. 2% and 3% of the base peak, respectively),[53,54] which is probably due to formation of stable fragment ions of $(CH_3CH{=}NH_2)^+$ ($m/z$ = 44) and $(CH_2{=}N(CH_3)_2)^+$ ($m/z$ = 58), corresponding to $(CH_2{=}NH_2)^+$ ($m/z$ = 30) for tryptamine, and of a stable indole chromophore. As shown in Table 1, a large enhancement factor of 28 was obtained for tryptamine. As a result, a molecular ion could be observed as one of the major peaks for both AMP and DMT via RE2PI, suggesting the superior performance of fs-LIMS in producing a molecular ion.

***N*-Methylephedrine.** Figure 8A shows the mass spectrum of *N*-methylephedrine measured by EIMS. Neither a molecular ion ($m/z$ = 179) nor large fragment ions were observed in EIMS. The most abundant peak at $m/z$ = 72 can be assigned to $(CH_3CH{=}N(CH_3)_2)^+$ produced from the molecular ion via one of the three types of cleavage of the $C_\alpha$–$C_\beta$ bond, as shown in Figure S25. It should be noted that this fragment ion is highly stabilized by the three $CH_3$ groups in the ion.

In fs-LIMS, a molecular ion was clearly observed at 280 nm, as shown in Figure 8B. This is a distinct advantage of fs-LIMS over EIMS in terms of observing a molecular ion, thus providing information concerning the molecular weight of the analyte. A $(C_6H_5{-}CO)^+$ ($m/z$ = 105) fragment ion was observed, in addition to a tropolonium cation ($m/z$ = 91), a benzene cation ($m/z$ = 77), and a pentadienyl cation ($m/z$ = 65), in fs-LIMS (see the fragmentation pathway shown in Figure S25). The dependence of the ratio, $M^+/F^+$ ($m/z$ = 105), on laser wavelength is shown in Figure 8C. The data shown in Figure S7 suggests that *N*-methylephedrine is ionized via NR2PI at <300 nm and at >300 nm in the case of NR3PI. The maximum of the ratio observed in Figure 8C can be explained by a small excess energy at 280 nm (0.56 = 8.86−8.30 eV) based on the IE value (8.30 eV) obtained by DFT.

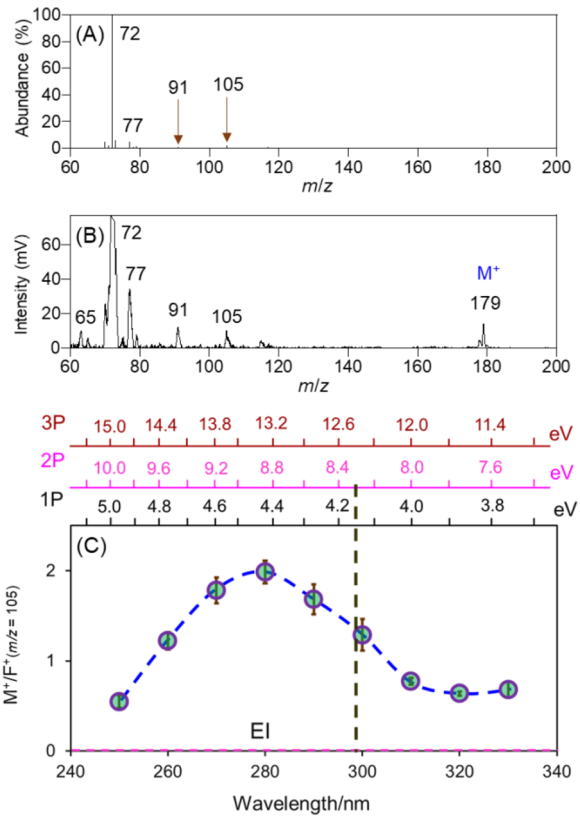


**Figure 8.** Mass spectral data for *N*-methylephedrine: (A) EIMS, (B) fs-LIMS measured at 280 nm, (C) ratio of signal intensities observed for a molecular ion, $M^+$, and a fragment ion, $(M - C_4H_{12}N)^+$ ($m/z$ = 105), at different wavelengths. The ratio obtained by EIMS is shown as a pink broken line. No data were available for IE measured by photoelectron spectroscopy. A fragment peak observed at $m/z$ = 105 (not a base peak) was used for comparison, since the base peak observed at $m/z$ = 72 went off the scale. Dark brown broken line: IE calculated by DFT.

*N*-Methylephedrine is an analogue of cathine. Note that no molecular ion is reported for these compounds in the NIST EIMS database.[55,56] This unfavorable result can be attributed to the formation of a stable ion of $(CH_3CH{=}N(CH_3)_2)^+$ ($m/z$ = 72) for *N*-methylephedrine and $(CH_3CH{=}NH_2)^+$ ($m/z$ = 44) for cathine (see Figures S25 and S26). It is noteworthy that a fragment ion at $m/z$ = 105 was reported for cathine in the NIST EIMS database and the fragmentation pathway is similar to that for *N*-methylephedrine, as shown in Figures S25 and S26. As a result, a molecular ion for cathine is likely observed in fs-LIMS, since the molecular ion observed for *N*-methylephedrine is 2 times larger than the fragment ion at $m/z$ = 105 in fs-LIMS.

**Nicotine.** Figure 9A shows the mass spectrum of nicotine measured by EIMS. A small molecular ion was observed at $m/z$ = 162, in addition to a fragment ion appeared at $m/z$ = 161 by the dissociation of a hydrogen atom. The fragmentation pathway is summarized in Figure S27. The peak at $m/z$ = 133 appeared as a result of a complex ring-opening reaction of an aliphatic heteroring structure. On the other hand, the base peak was observed at $m/z$ = 84 by cleavage of the $C_\alpha$–$C_\beta$ bond combining two heterocyclic rings. This fragment ion is further dissociated into smaller fragment ions at $m/z$ = 65 and 42 (see


https://doi.org/10.1021/jasms.1c00282
J. Am. Soc. Mass Spectrom. 2022, 33, 90−99

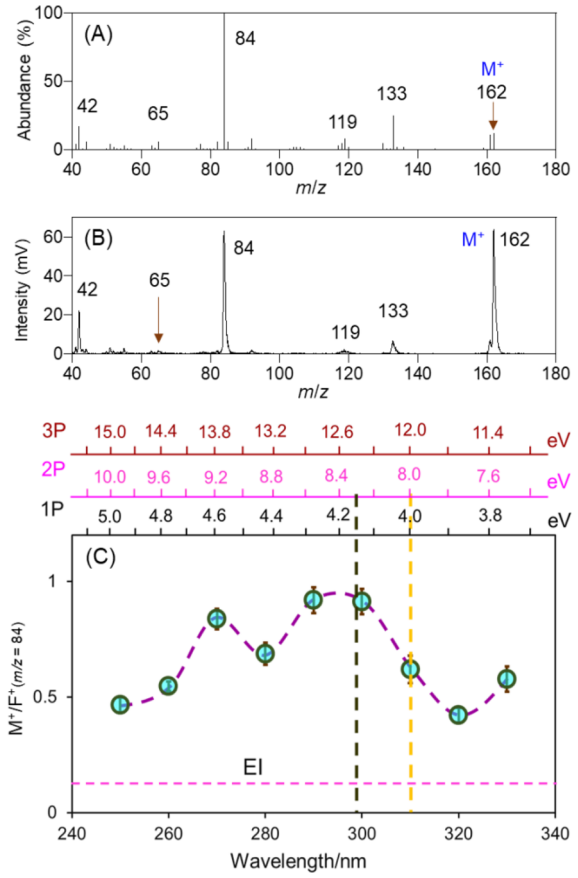


**Figure 9.** Mass spectral data for nicotine: (A) EIMS, (B) fs-LIMS measured at 290 nm, (C) ratio of the signal intensities observed for a molecular ion, $M^+$, and a fragment ion, $(C_5H_{10}N)^+$ ($m/z$ = 84), at different wavelengths. The ratio obtained by EIMS is shown as a pink broken line. Yellow broken line: IE measured by photoelectron spectroscopy. Dark brown broken line: IE calculated by DFT.

Figure S27). These signal peaks are important in terms of identifying nicotine and its related compounds.

In fs-LIMS, the intensity of the molecular ion ($m/z$ = 162) was nearly identical to that of the $m/z$ = 84 peak when observed at 290 nm, as shown in Figure 9B. As shown in Table 1, an enhancement factor of 7.8 was obtained for nicotine. The other peaks observed at $m/z$ = 161 and 133 were suppressed in fs-LIMS. The dependence of the $M^+/F^+$ ($m/z$ = 84) ratio on the laser wavelength is shown in Figure 9C. The IE value for nicotine is reported to be 8.23 eV,[57] which is close to the calculated value of 8.41 eV by DFT. As a result, nicotine can be ionized via two-photon ionization (2PI) at <310 nm, the excess energy being calculated to be 0.31 eV (= 8.54−8.23 eV) at 290 nm. At wavelengths longer than 310 nm, nicotine is ionized via 3PI and the excess energy is increased substantially to 3.77 eV (= (4.0 × 3) − 8.23 eV) at 310 nm. Therefore, a large ratio observed at 290 nm can be attributed to a smaller excess energy in the ionic state via 2PI. It is interesting to note that another maximum appeared at 270 nm. This result can be explained by a contribution of RE2PI since the molar absorptivity increases at wavelengths shorter than 270 nm (see Figure S9).

Nicotine is a cyclic amine with a rigid chemical structure, providing a molecular ion even in EIMS. However, it easily dissociates to form a fragment ion of $(M - 1)^+$, and the molecular ion should be more carefully identified. This is in contrast to the data obtained by fs-LIMS, providing a molecular ion as a base peak in the mass spectrum.

## CONCLUSIONS

Amine-related psychoactive substances of amphetamine/methylamphetamine, MDA/MDMA, AMT/DMT, and cathine, in addition to nicotine, were investigated using phenethylamine, 3,4-methylenedioxyphenethylamine, tryptamine, and *N*-methylephedrine as analogues, by GC−TOFMS using a tunable femtosecond UV laser as the ionization source. A nonbonding lone pair of electrons on the nitrogen atom can easily be emitted with the formation of a molecular ion, which is followed by the cleavage of the N−$C_\alpha$ and/or $C_\alpha$−$C_\beta$ bond and a rearrangement of the chemical structure. As a result, a small or sometimes no molecular ion signal is observed in EIMS. When the complete data about the retention time and the mass spectrum are available in the database, it is possible to assign the analyte of interest. However, new types of illegal psychoactive substances are synthesized every year, and standards are not available, even in the research laboratory. As a result, it would be difficult to reconstruct the chemical structure of such an analyte from the observed data. In fs-LIMS, a molecular ion as well as large fragment ions were observed and provided more information-rich mass spectra. In fact, the relative signal intensity of the molecular ion against the base ion peak was enhanced (>7.8−28-fold) by using fs-LIMS. Accordingly, the chemical structure of the molecule can be predicted, even for unknown psychoactive substances, from the molecular ion, thus providing a molecular weight and the large fragment ions providing partial chemical structures. Needless to say, additional spectroscopic techniques based on VUV, IR, and NMR are of importance for more reliable and accurate assignment of the compounds. The molecular ion can be enhanced in the spectral region of 260−310 nm (5−20 mW). The third harmonic emission (267 nm) with a larger output power (500 mW) will be useful for more sensitive detection of psychoactive substances and other organic compounds as well, since the signal intensity increases in proportion to the square of the output power. It is noted that a small mass spectrometer consisting of a low-price femtosecond laser and a compact mass analyzer has been developed in our laboratory, which will be potentially useful for practical trace analysis of amine-related psychoactive substances in the future.

## ASSOCIATED CONTENT

### Supporting Information

The Supporting Information is available free of charge at https://pubs.acs.org/doi/10.1021/jasms.1c00282.

Absorption spectrum for neutral molecule of phenethylamine: absorption spectrum for molecular ion of phenethylamine: absorption spectrum for neutral molecule of 3,4-methylenedioxyphenethylamine: absorption spectra for molecular ion of 3,4-methylenedioxyphenethylamine; absorption spectrum for neutral molecule of tryptamine; absorption spectrum for molecular ion of tryptamine: absorption spectrum for neutral molecule of *N*-methylephedrine; absorption spectrum for molecular ion of *N*-methylephedrine; absorption spectrum for neutral molecule of nicotine; absorption spectrum for molecular ion of nicotine: two-dimensional display of GC−MS for a sample mixture containing *N*-methylephedrine and nicotine: mass



https://doi.org/10.1021/jasms.1c00282
J. Am. Soc. Mass Spectrom. 2022, 33, 90−99

spectra of phenethylamine measured at different laser wavelengths; mass spectra of 3,4-methylenedioxyphenethylamine measured at different laser wavelengths; mass spectra of tryptamine measured at different laser wavelengths; mass spectra of *N*-methylephedrine measured at different laser wavelengths; mass spectra of nicotine measured at different laser wavelengths; possible pathway of fragmentation at positions of $C_\alpha$–$C_\beta$ and $C_\alpha$–N bonds for phenethylamine; possible pathway of fragmentation at positions of $C_\alpha$–$C_\beta$ and $C_\alpha$–N bonds for amphetamine; possible pathway of fragmentation at positions of $C_\alpha$–$C_\beta$ and $C_\alpha$–N bonds for methylamphetamine; possible pathway of fragmentation at positions of $C_\alpha$–$C_\beta$ and $C_\alpha$–N bonds for 3,4-methylenedioxyphenethylamine; possible pathway of fragmentation at positions of $C_\alpha$–$C_\beta$ and $C_\alpha$–N bonds for MDMA; possible pathway of fragmentation at positions of $C_\alpha$–$C_\beta$ and $C_\alpha$–N bonds for tryptamine; possible pathway of fragmentation at positions of $C_\alpha$–$C_\beta$ and $C_\alpha$–N bonds for AMT; possible pathway of fragmentation at positions of $C_\alpha$–$C_\beta$ and $C_\alpha$–N bonds for DMT; possible pathway of fragmentation at positions of $C_\alpha$–$C_\beta$ and $C_\alpha$–N bonds for *N*-methylephedrine; possible pathway of fragmentation at positions of $C_\alpha$–$C_\beta$ and $C_\alpha$–N bonds for cathine; possible pathway of fragmentation at positions of $C_\alpha$–$C_\beta$ and $C_\alpha$–N bonds for nicotine (PDF)

## AUTHOR INFORMATION


### Corresponding Author

**Tomoko Imasaka** − *Faculty of Design, Kyushu University, Fukuoka 819-0395, Japan;* orcid.org/0000-0002-2131-4995; Email: imasaka@design.kyushu-u.ac.jp

### Authors

**Siddihalu Lakshitha Madunil** − *Faculty of Design, Kyushu University, Fukuoka 819-0395, Japan*

**Totaro Imasaka** − *Kyushu University, Fukuoka 819-0395, Japan; Hikari Giken, Co., Fukuoka 810-0024, Japan*

Complete contact information is available at: https://pubs.acs.org/10.1021/jasms.1c00282


### Author Contributions

Siddihalu Lakshitha Madunil performed the experimental work and wrote the original draft. Totaro Imasaka supervised the work and revised the draft. Tomoko Imasaka acquired funding, supervised the work, and performed computational calculations.

### Notes

The authors declare no competing financial interest.

## ACKNOWLEDGMENTS

This research was supported by a Grant-in-Aid for Scientific Research from the Japan Society for the Promotion of Science (JSPS KAKENHI Grant No. 20H02399) and by the Program of Progress 100 in Kyushu University, The Iwatani Naoji Foundation, 2020 Collaboration Development Fund for Joint Program between National Taiwan Normal University and Kyushu University, and Heiwa Nakajima Foundation. Quantum chemical calculations were mainly carried out using the computer facilities at the Research Institute for Information Technology, Kyushu University. We thank Prof. Noriyuki Igura for the use of the GC−EIMS in the Faculty of Agriculture, Kyushu University. S.L.M. acknowledges the Mitsubishi Corporation International Scholarship for financial support to study in Japan.

## REFERENCES


(1) United Nations Office on Drugs and Crime. World Drug Report: Drug use and health consequences 2020, https://wdr.unodc.org/wdr2020/en/drug-use-health.html.

(2) United Nations Office on Drugs and Crime. *Convention on psychotropic substances* 1971, https://www.unodc.org/pdf/convention_1971_en.pdf (last accessed 2020-09).

(3) Roberson, Z. R.; Goodpaster, J. V. Differentiation of structurally similar phenethylamines via gas chromatography-vacuum ultraviolet spectroscopy (GC-VUV). *Forensic Chem.* **2019**, *15*, 100172.

(4) Kranenburg, R. F.; García-Cicourel, A. R.; Kukurin, C.; Janssen, H.-G.; Schoenmakers, P. J.; van Asten, A. C. Distinguishing drug isomers in the forensic laboratory: GC−VUV in addition to GC−MS for orthogonal selectivity and the use of library match scores as a new source of information. *Forensic Sci. Int.* **2019**, *302*, 109900.

(5) Kranenburg, R. F.; Lukken, C. K.; Schoenmakers, P. J.; van Asten, A. C. Spotting isomer mixtures in forensic illicit drug casework with GC−VUV using automated coelution detection and spectral deconvolution. *J. Chromatogr. B: Anal. Technol. Biomed. Life Sci.* **2021**, *1173*, 122675.

(6) Kalasinsky, K. S.; Levine, B.; Smith, L. M.; Platoff, G. E., Jr. Comparison of infrared and mass spectroscopies for drug analysis. *Crit. Rev. Anal. Chem.* **1993**, *23*, 441−457.

(7) DeRuiter, J.; Smith, F.; Abiedalla, Y.; Neel, L.; Clark, C. R. GC-MS and GC-IR analysis of regioisomeric cannabinoids related to 1-(5-fluoropentyl)-3-(1-naphthoyl)-indole. *Forensic Chem.* **2018**, *10*, 48−57.

(8) Rösner, P.; Quednow, B.; Girreser, U.; Junge, T. Isomer fluoro-methoxy-phenylalkylamines: a new series of controlled-substance analogues (designer drugs). *Forensic Sci. Int.* **2005**, *148*, 143−156.

(9) O'Brien, E.; Nic Daeid, N.; Black, S. Science in the court: pitfalls, challenges and solutions. *Philos. Trans. R. Soc., B* **2015**, *370*, 20150062.

(10) Maralikova, B.; Weinmann, W. Confirmatory analysis for drugs of abuse in plasma and urine by high-performance liquid chromatography−tandem mass spectrometry with respect to criteria for compound identification. *J. Chromatogr. B: Anal. Technol. Biomed. Life Sci.* **2004**, *811*, 21−30.

(11) Rocchi, R.; Simeoni, M. C.; Montesano, C.; Vannutelli, G.; Curini, R.; Sergi, M.; Compagnone, D. Analysis of new psychoactive substances in oral fluids by means of microextraction by packed sorbent followed by ultra-high-performance liquid chromatography−tandem mass spectrometry. *Drug Test. Anal.* **2018**, *10*, 865−873.

(12) Luo, Y.; Du, J.; Xiao, H.; Zheng, L.; Chen, X.; Ma, A.; Luo, Q. Simultaneous determination of methamphetamine and its isomer N-isopropylbenzylamine in forensic samples by using a modified LC-ESI-MS/MS method. *J. Nanomater.* **2021**, *2021*, 6679515.

(13) Chikumoto, T.; Kadomura, N.; Matsuhisa, T.; Kawashima, H.; Kohyama, E.; Nagai, H.; Soda, M.; Kitaichi, K.; Ito, T. Differentiation of FUB-JWH-018 positional isomers by electrospray ionization−triple quadrupole mass spectrometry. *Forensic Chem.* **2019**, *13*, 100157.

(14) Smolianitski-Fabian, E.; Cohen, E.; Dronova, M.; Voloshenko-Rossin, A.; Lev, O. Discrimination between closely related synthetic cannabinoids by GC−Cold−EI−MS. *Drug Test. Anal.* **2018**, *10*, 474−487.

(15) Levitas, M. P.; Andrews, E.; Lurie, I.; Marginean, I. Discrimination of synthetic cathinones by GC−MS and GC−MS/MS using cold electron ionization. *Forensic Sci. Int.* **2018**, *288*, 107−114.

(16) Amirav, A.; Neumark, B.; Eren, K. J. M.; Fialkov, A. B.; Tal, N. Cannabis and its cannabinoids analysis by gas chromatography−mass spectrometry with cold EI. *J. Mass Spectrom.* **2021**, *56*, e4726.

(17) Kranenburg, R. F.; Peroni, D.; Affourtit, S.; Westerhuis, J. A.; Smilde, A. K.; van Asten, A. C. Revealing hidden information in GC−MS spectra from isomeric drugs: Chemometrics based identification from 15 and 70 eV EI mass spectra. *Forensic Chem.* **2020**, *18*, 100225.
(18) Imasaka, T. Gas chromatography/multiphoton ionization/time-of-flight mass spectrometry using a femtosecond laser. *Anal. Bioanal. Chem.* **2013**, *405*, 6907−6912.
(19) Imasaka, T.; Imasaka, T. Femtosecond ionization mass spectrometry for chromatographic detection. *J. Chromatogr. A* **2021**, *1642*, 462023.
(20) Dela Cruz, J. M.; Lozovoy, V. V.; Dantus, M. Quantitative mass spectrometric identification of isomers applying coherent laser control. *J. Phys. Chem. A* **2005**, *109*, 8447−8450.
(21) Zhu, X.; Lozovoy, V. V.; Shah, J. D.; Dantus, M. Photodissociation dynamics of acetophenone and its derivatives with intense nonresonant femtosecond pulses. *J. Phys. Chem. A* **2011**, *115*, 1305−1312.
(22) Schäfer, V.; Weitzel, K.-M. Qualitative and quantitative distinction of ortho-, meta-, and para-fluorotoluene by means of chirped femtosecond laser ionization. *Anal. Chem.* **2020**, *92*, 5492−5499.
(23) Reusch, N.; Krein, V.; Wollscheid, N.; Weitzel, K.-M. Distinction of structural isomers of benzenediamin and difluorobenzene by means of chirped femtosecond laser ionization mass spectrometry. *Z. Phys. Chem.* **2018**, *232*, 689−703.
(24) Zimmermann, R.; Welthagen, W.; Gröger, T. Photo-ionisation mass spectrometry as detection method for gas chromatography: Optical selectivity and multidimensional comprehensive separations. *J. Chromatogr. A* **2008**, *1184*, 296−308.
(25) Phan, T. D.; Li, A.; Nakamura, H.; Imasaka, T.; Imasaka, T. Single-photon ionization mass spectrometry using a vacuum ultraviolet femtosecond laser. *J. Am. Soc. Mass Spectrom.* **2020**, *31*, 1730−1737.
(26) Finch, J. W.; Toerne, K. A.; Schram, K. H.; Denton, M. B. Evaluation of a hydrogen laser vacuum ultraviolet source for photoionization mass spectrometry of pharmaceuticals. *Rapid Commun. Mass Spectrom.* **2005**, *19*, 15−22.
(27) Matsumoto, J.; Lin, C. H.; Imasaka, T. Enhancement of the molecular ion peak from halogenated benzenes and phenols using femtosecond laser pulses in conjunction with supersonic beam/multiphoton ionization mass spectrometry. *Anal. Chem.* **1997**, *69*, 4524−4529.
(28) Li, A.; Uchimura, T.; Tsukatani, H.; Imasaka, T. Trace analysis of polycyclic aromatic hydrocarbons using gas chromatography−mass spectrometry based on nanosecond multiphoton ionization. *Anal. Sci.* **2010**, *26*, 841−846.
(29) Kouno, H.; Imasaka, T. The efficiencies of resonant and nonresonant multiphoton ionization in the femtosecond region. *Analyst* **2016**, *141*, 5274−5280.
(30) Madunil, S. L.; Imasaka, T.; Imasaka, T. Resonant and nonresonant femtosecond ionization mass spectrometry of organochlorine pesticides. *Analyst* **2020**, *145*, 777−783.
(31) Mullen, C.; Huestis, D.; Coggiola, M.; Oser, H. Laser photoionization of triacetone triperoxide (TATP) by femtosecond and nanosecond laser pulses. *Int. J. Mass Spectrom.* **2006**, *252*, 69−72.
(32) Hamachi, A.; Okuno, T.; Imasaka, T.; Kida, Y.; Imasaka, T. Resonant and nonresonant multiphoton ionization processes in the mass spectrometry of explosives. *Anal. Chem.* **2015**, *87*, 3027−3031.
(33) Madunil, S. L.; Imasaka, T.; Imasaka, T. Suppression of fragmentation in mass spectrometry. *Anal. Chem.* **2020**, *92*, 16016−16023.
(34) Matsui, T.; Fukazawa, K.; Fujimoto, M.; Imasaka, T. Analysis of persistent organic pollutants at sub-femtogram levels using a high-power picosecond laser in gas chromatography/multiphoton ionization/time-of-flight mass spectrometry. *Anal. Sci.* **2012**, *28*, 445−450.
(35) Gross, J. H. Chemical Ionization. In *Mass spectrometry*, 2nd ed.; Springer-Verlag: Heidelberg, 2004; pp 341−344.
(36) Pavia, D. L.; Lampman, G. M.; Kriz, G. S. Mass Spectrometry. In *Introduction to Spectroscopy*, 3rd ed.; Thomson Learning, 2001; pp 390−465.
(37) Baer, T. Photoelectron−photoion coincidence methods in mass spectrometry (PEPICO). In Encyclopedia of Spectroscopy and Spectrometry. *Elsevier* **1999**, 1831−1839.
(38) Hemberger, P.; Trevitt, A. J.; Ross, E.; da Silva, G. Direct observation of para-xylylene as the decomposition product of the meta-xylyl radical using VUV synchrotron radiation. *J. Phys. Chem. Lett.* **2013**, *4*, 2546−2550.
(39) Bauernschmitt, R.; Ahlrichs, R. Treatment of electronic excitations within the adiabatic approximation of time dependent density functional theory. *Chem. Phys. Lett.* **1996**, *256*, 454−464.
(40) National Institute of Standards and Technology. https://webbook.nist.gov/cgi/cbook.cgi?ID=C96093&Units=SI&Mask=200#Mass-Spec (accessed 2021-02-25).
(41) Chen, B. H.; Liu, J. T.; Chen, W. X.; Chen, H. M.; Lin, C. H. A general approach to the screening and confirmation of tryptamines and phenethylamines by mass spectral fragmentation. *Talanta* **2008**, *74*, 512−517.
(42) Domelsmith, L. N.; Munchausen, L. L.; Houk, K. N. Photoelectron spectra of psychotropic drugs. 1. Phenethylamines, tryptamines, and LSD. *J. Am. Chem. Soc.* **1977**, *99*, 4311−4321.
(43) National Institute of Standards and Technology. https://webbook.nist.gov/cgi/cbook.cgi?ID=C300629&Mask=200 (accessed 2021-02-01).
(44) National Institute of Standards and Technology. https://webbook.nist.gov/cgi/cbook.cgi?ID=C537462&Mask=200 (accessed February 01, 2021).
(45) National Institute of Standards and Technology. https://webbook.nist.gov/cgi/cbook.cgi?ID=C7145995&Units=SI&Mask=200#Mass-Spec (accessed 2021-02-24).
(46) National Institute of Standards and Technology. https://webbook.nist.gov/cgi/cbook.cgi?ID=C591311&Units=SI&Mask=200#Mass-Spec (accessed 2021-02-24).
(47) National Institute of Standards and Technology. https://webbook.nist.gov/cgi/cbook.cgi?ID=42542-10-9&Units=SI&cMS=on (accessed 2021-02-01).
(48) National Institute of Standards and Technology. https://webbook.nist.gov/cgi/cbook.cgi?ID=C61507&Units=SI&Mask=200#Mass-Spec (accessed 2021-03-17).
(49) National Institute of Standards and Technology. https://webbook.nist.gov/cgi/cbook.cgi?ID=C299263&Units=SI&Mask=200#Mass-Spec (accessed 2021-03-17).
(50) National Institute of Standards and Technology. https://webbook.nist.gov/cgi/cbook.cgi?ID=C83341&Units=SI&Mask=200#Mass-Spec (accessed 2021-03-17).
(51) National Institute of Standards and Technology. https://webbook.nist.gov/cgi/cbook.cgi?ID=C95205&Units=SI&Mask=200#Mass-Spec (accessed 2021-03-17).
(52) National Institute of Standards and Technology. https://webbook.nist.gov/cgi/cbook.cgi?ID=C120729&Mask=400#UV-Vis-Spec (accessed 2021-02-01).
(53) National Institute of Standards and Technology. https://webbook.nist.gov/cgi/cbook.cgi?ID=299-26-3&Units=SI&cMS=on (accessed 2021-02-01).
(54) National Institute of Standards and Technology. https://webbook.nist.gov/cgi/cbook.cgi?ID=C61507&Mask=200 (accessed 2021-02-01).
(55) National Institute of Standards and Technology. https://webbook.nist.gov/cgi/cbook.cgi?ID=C552794&Units=SI&Mask=200#Mass-Spec (accessed 2021-02-01).
(56) National Institute of Standards and Technology. https://webbook.nist.gov/cgi/cbook.cgi?ID=C492397&Mask=200 (accessed 2021-02-01).
(57) Kuhn, W. F.; Lilly-Leister, D.; Kao, J.; Lilly, A. C. Comparison of theoretical and experimental ionization potentials of nicotine and related molecules. *J. Mol. Struct.* **1989**, *212*, 37−44.


https://doi.org/10.1021/jasms.1c00282
J. Am. Soc. Mass Spectrom. 2022, 33, 90−99